PREPARED FOR THE U.S. DEPARTMENT OF ENERGY,
UNDER CONTRACT DE-AC02-76CH03073

PPPL-3503rev
UC-70

PPPL-3503rev

The Combined Effect of EPM and TAE Modes on Energetic Ion Confinement and Sawtooth Stabilization

by

S. Bernabei, R. Budny, E.D. Fredrickson, N.N. Gorelenkov, J.C. Hosea,
C.K. Phillips, R. White, J.R. Wilson, C.C. Petty, R.I. Pinsker,
R.W. Harvey, and P. Smirnov

Revised May 2001

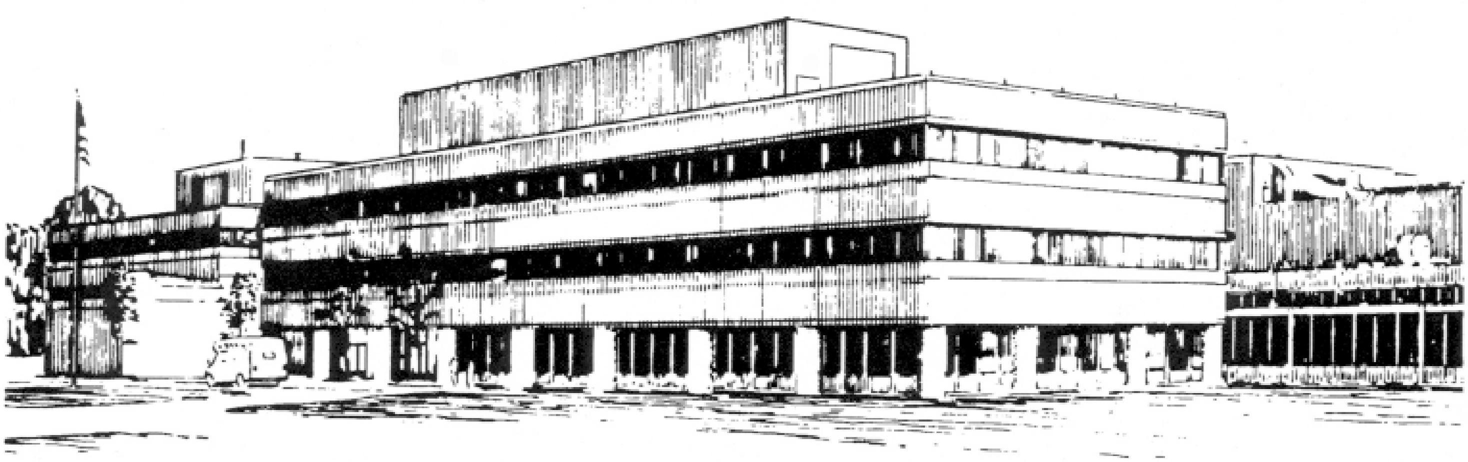

PRINCETON PLASMA PHYSICS LABORATORY
PRINCETON UNIVERSITY, PRINCETON, NEW JERSEY

Availability

This report is posted on the U.S. Department of Energy's Princeton Plasma Physics Laboratory Publications and Reports web site in Calendar Year 2001. The home page for PPPL Reports and Publications is: http://www.pppl.gov/pub_report/

DOE and DOE Contractors can obtain copies of this report from:

U.S. Department of Energy
Office of Scientific and Technical Information
DOE Technical Information Services (DTIS)
P.O. Box 62
Oak Ridge, TN 37831

Telephone: (865) 576-8401

Fax: (865) 576-5728

Email: reports@adonis.osti.gov

This report is available to the general public from:

National Technical Information Service
U.S. Department of Commerce
5285 Port Royal Road
Springfield, VA 22161

Telephone: 1-800-553-6847 or
(703) 605-6000

Fax: (703) 321-8547

Internet: http://www.ntis.gov/ordering.htm

THE COMBINED EFFECT OF EPM AND TAE MODES ON ENERGETIC ION CONFINEMENT AND SAWTOOTH STABILIZATION

S. BERNABEI, R. BUDNY, E. D. FREDRICKSON, N. N. GORELENKOV,
J. C. HOSEA, C. K. PHILLIPS, R. WHITE, J. R. WILSON,
Princeton Plasma Physics Laboratory, Princeton N.J. 08540
C. C. PETTY, R. I. PINSKER,
General Atomics, San Diego, California 92186
R. W. HARVEY,
CompX, P.O. Box 2672, Del Mar, California 92014
P. SMIRNOV
Moscow State University, Moscow, Russia.

ABSTRACT. It is shown in this paper for the first time, that the chirping Alfvén instabilities observed mostly during ICRF heating have been positively identified as Energetic Particle Modes. This has been possible because of the detailed measurement of the q-profile with the MSE diagnostic in DIII-D. The EPMs are shown to be the leading cause of the monster sawtooth crash. It is also shown that TAEs are excited either directly or indirectly by the EPMs and they cause fast ion losses. A scenario for the stabilization and the crash of the monster sawtooth and for the degradation of the ICRF heating efficiency at high power is presented.

INTRODUCTION.

It has been reported in several experiments that sawteeth are transiently stabilized by a hot ion component of the ion energy distribution function inside r(q=1)[1]. These so-called giant sawteeth crash because of a depletion of fast ions from the core. In the TFTR experiment, TAE modes were found to expel ions to the plasma edge and Energetic Particle Modes in the plasma core were shown to be the catalyst for expulsion of energetic ions from the core, using TRANSP [2] for modeling the equilibrium and HINST[3] for the instabilities[4].

A similar experiment was performed on DIII-D. With an equilibrium constrained by the experimentally measured q-profile, it has been possible to uniquely identify the Alfvén instabilities causing the expulsion of ions from inside the q=1 radius as EPMs [5]. Using the results from DIII-D, supplemented by similar results on TFTR, a consistent scenario has emerged in which it is found that the EPMs initiate the radial transport of fast ions to the plasma boundary, causing the giant sawtooth crash. The subsequent appearance of TAEs causes heavy losses of fast ions and the familiar drop below offset linear of the stored energy versus the injected RF power. This scenario does not require the production of “potato” orbits which have been suggested as the cause of the loss of fast ion energy at higher RF powers [6].

SAWTOOTH STABILIZATION.

Unlike other Ion Cyclotron Range of Frequency heating (ICRF) experiments, in DIII-D the fast ion component of the distribution function is not generated by fundamental or second harmonic acceleration of a minority ion species, but by higher harmonic acceleration of the existing fast ions injected via Neutral Beam Injection (NBI).

When the cyclotron resonance is placed near the center of the plasma the resultant fast ion distribution can transiently stabilize the sawtooth. “Monster” sawteeth of up to 300 msec between crashes can be obtained. The monster sawtooth is always accompanied by Alfvén instabilities that terminate with the sawtooth crash [figure 1]. As observed in TFTR, there are two kinds of sawteeth, short and long, but none with an intermediate length of the period, indicating that only if the fast ion pressure grows fast enough there is transient stabilization. When the fast ion density becomes high enough the Alfvén instabilities grow inducing particle loss and the sawtooth crash.

Shifting the resonance layer away from the axis prevents the formation of the monster sawtooth (see figure 2). Comparing the DIII-D frequency spectrum of the Alfvén instabilities with those observed in TFTR, it appears that at the modest power level in DIII-D the RF power is just above the minimum threshold for stabilization and formation of monster sawteeth.

The CQL3D [7] code has been used to calculate the radial profile of the damping of the injected ICRF power and the self-consistent quasi-linear diffusion of the neutral beam-injected ions. It has been found that bulk of the damping occurs at the 4th harmonic resonant location of Deuterium when it is placed on axis, with some power deposited at the location of the 3rd and 5th harmonics and some directly into the electrons. $4\Omega_D$ resonance location off-axis results in a weaker tail, not sufficient for stabilizing the sawtooth and in this case the Alfvén instabilities are not excited. Figure 3 shows the damping calculated by CQL3D for a discharge (96467) with the $4\Omega_D$ resonance near the plasma axis, slightly on the high field side (B=18.7kG) and for a discharge (96492) with the resonance well off-axis (B=20.6kG). The code uses a zero-banana width approximation. The finite banana width effect will spread the distribution of particles.

Considering that the fast ion profile generated by NBI is centered on axis, the shift of the IC resonance is sufficient to produce fewer fast ions in the core. To verify this experimentally, the fast ion component created by the ICRF is determined by subtracting the beam ion pressure, calculated with ONETWO transport code [8], from the total ion pressure and a magnetic equilibrium reconstruction with MSE data [9]. (figure 4) With the resonance near the plasma axis, ICRF creates a stronger population of fast ions: this explains the stabilization of the sawtooth. As it will be seen in the next section, the same fast ion distribution is sufficient to destabilize core localized Alfvén modes in the first case, and insufficient for the off-axis case.

EPMs AND THE SAWTOOTH CRASH.

The HINST code has been used to model the Alfvén instabilities that accompany the monster sawtooth since it is a fully kinetic non-perturbative code. A key element for the identification of these modes as Energetic Particle Modes (EPM) is the use of the experimental q-profile. The MSE diagnostic on DIII-D has provides accurate q-profile data which now permit an even more compelling identification of the modes than obtained for the TFTR results which had to rely on the TRANSP reconstruction of the evolution of the q-profile [4].

With the plasma beta observed in the DIII-D experiment, $\beta(0)$=4.4 %, the HINST analysis predicts the mode to be inside the lower continuum, similar to the result reported in [4]. Using the measured evolution of the q-profile, the chirping of the modes has been equally well duplicated (fig. 5). Correspondingly, because of the strong damping due to the high beta value, NOVA-K [10], being an ideal MHD code, failed to find a mode in the gap. The same modeling has been performed for discharge 96492, using the fast ion profile shown in figure 4. In this case HINST predicts the absence of any mode, in agreement with the experimental measurement.

Due to the low shear near the plasma center and medium toroidal mode numbers predicted, HINST can not resolve the radial EPM mode structure. To predict the mode structure, the plasma beta in the code was lowered to such a value that the EPM frequency was predicted to fall in the gap, and the mode is predicted to transform into a core localized TAE. This occurred when $\beta(0)$ was lowered to 1.5%. NOVA was then used to calculate the radial structure of the EPM, as shown in figure 6. For further analysis we will assume that the EPM and core localized TAE mode structures are alike.

The calculated mode has n=6 (n is the toroidal mode number), like the observed mode at t=2030 msec, and f=230 kHz. After taking into account the toroidal plasma rotation of ~5 kHz, the Doppler shifted frequency of f=260 kHz is in very good agreement with the experimental one (see figure 1).

The EPMs are core-localized eigenmodes, which reside in the Alfvén continuum at a location determined by the minor axis where $q=q_{TAE}\approx 1-1/2n$ (n is the toroidal wave number). Thus as the central q, q_o, decreases in time due to resistive current diffusion, the EPM location moves radially outward and the fast ions are transported with the mode. This depletion of fast ions from the core results in the monster sawtooth crash when the energetic ion population contained within the q=1 surface becomes insufficient to stabilize the m=1 internal kink. It should be noted that as a mode with a certain toroidal number (n) has shifted outward, a new one with (n-1) is destabilized and acts in the same way on the newly formed fast ion tail as the previous one. In some cases in TFTR modes with n=10 down to n=4 have been observed.

The effect of the EPM modes on the ICRF particle distribution was simulated using the guiding center code ORBIT [11,12]. The mode structure, frequency and harmonic content were taken to be that given by NOVA-K code (fig. 6) while the initial particle distribution was given by Monte-Carlo generation using the deposition profile generated by CQL3D and spread by finite orbit effects (fig.3a). The mode amplitude was taken to be 10^{-4} B_θ/B, which is approximately that indicated by the experiment and by the NOVA-K results. One thousand test particles were followed for 100 msec, and in this time the location of the mode peak moved from r/a= 0.1 to r/a = 0.3, as indicated by the experimental evolution of the q profile. As seen in fig. 7 there is a significant broadening of the ICRF distribution produced in this time.

It is possible to see experimentally a progressive depletion of fast ions in the core with a shift of the distribution radially outward (fig. 8) by using the same technique applied to obtain the radial profile of the fast ion distribution at different times before the sawtooth crash. Comparing figs. 7 and 8 it is possible to see that the radial shift of the fast ion pressure is in qualitative agreement with the theoretical expectation.

EXCITATION OF TAE: TOTAL ENERGY vs. RF POWER.

In several experiments, most notably in TFTR, global TAEs are excited together with the EPMs. In experiments with high q_a the TAE gap is aligned: in this case the global modes extend to the plasma core and TAE are excited directly by the ICRF driven hot ions [4]. At low q_a there are essentially two situations for the destabilization of TAEs. As shown in reference [4] TAE can be excited by the flow of fast particles redistributed from the core by the EPM (and in few cases by sawteeth). This happens without direct coupling of the EPM and TAE frequencies. In addition, in reference [13] it was shown that coupling between unstable “core” modes (like EPMs) and stable “global” modes (TAEs) is possible when

$$f_{EPM} \approx f_{TAE} \text{ and } n_{EPM} = n_{TAE}.$$

This happens when the frequency of the EPM decreases to match the TAE frequency near the edge of the plasma. Figure 9 (TFTR) gives the EPM and TAE spectra and a coupling of the two modes appears likely where the mode frequencies converge, taking into account the matching toroidal numbers. In TFTR, the appearance of TAE follows the appearance of EPM [14]: when the two modes are present very strong fast ion losses are registered by the “lost alphas” probes [14]. Similar modeling with ORBIT to the one shown in the preceding section has been performed with multiple overlapping global TAE. The two loss mechanisms induced by the TAE are resonance causing the orbit to lose energy and become trapped, the large banana hitting near the outer midplane, and the diffusion outwards of trapped orbits. The combination of core EPM and global TAE provides a diffusion of the fast ions all the way to the edge of the plasma.

Looking at the total energy of the plasma during ICRF heating, three phases are clearly discernible at increasing RF power:

A. At first E_{TOT} increases linearly with RF power: the fast ions are produced but the hot beta is too low to cause sawtooth stabilization.
B. As the RF power is increased, the fast ion distribution grows: this distribution is sufficient to stabilize the sawtooth, but it also destabilizes the EPM, causing the monster sawtooth crash. In this region, the increase of E_{TOT} diminishes slightly and the lost alpha probe begins to detect fast ions.
C. As soon as the power is such that in addition to EPM also TAE are destabilized, a diffusion channel is produced from the core all the way to the edge. Losses greatly increase as evidenced by the lost alpha probes and rate of increase of E_{TOT} is greatly diminished. (figure 10).

Therefore, by comparing the DIII-D data to the TFTR data, it appears that in DIII-D the RF power is sufficient to destabilize the EPM, but it is still below threshold for the coupling to TAEs.

CONCLUSIONS.

In conclusion, by making use of the q-profile measured in DIII-D it has been possible to uniquely identify the core modes which accompany the monster sawteeth as

Energetic Particle Modes. The overall scenario which results is one in which the ICRF accelerated fast ions stabilize the sawtooth, then destabilize the EPM which transport radially the fast ions causing the monster crash. Further transport by the TAE causes the loss of the fast particles and the degradation of the core ICRF heating efficiency.

These results can be generalized to any experiment which involves the production of fast particles in the core: it is found [4] that the first necessary condition for the confinement of fast particles in a conventional Tokamak is to confine the TAEs to the edge of the plasma. This occurs in low q_a discharges, since the Alfvén gap tends to "close" at low q_a. Second, it is necessary to keep the EPMs separate from the TAEs, that is prevent their shifting radially. Since the radial shift accompanies the decreasing q_0, it is necessary freeze the q-profile. This can be obtained with proper current drive, like central counter ECCD.

FIGURE CAPTIONS.

Fig. 1 Monster sawtooth with accompanying Alfvén instabilities in DIII-D. RF power of 1.2 MW is applied at t= 1800 msec.

Fig.2 Sawtooth period versus magnetic field strength: at B=19 kG the cyclotron resonance is on the magnetic axis.

Fig. 3 CQL3D modeling of the damping of the ICRF waves in two shots differing in magnetic field. 96467 at B=18.7 kG (a), 96492 at B=20.6 kG (b).

Fig.4 RF induced fast ions profiles determined experimentally for the two discharges of figure 3.

Fig.5 Variation of the EPM frequency calculated by HINST, normalized to the value of the central Alfvén frequency at q_0=0.9, vs. decreasing q_0.

Fig. 6 NOVA calculation for the radial mode structure excited by the fast ion distribution of figure 4 (shot 96467). The plasma displacement component with the dominant poloidal harmonic l=5,6 is plotted versus $\sqrt{\Psi}$ ~ r/a

fig. 7 Normalized distribution of fast ions vs. radius, calculated by ORBIT code at the onset of the EPM (dotted line) and just before the sawtooth crash. DIII-D shot 96467.

Fig.8 Experimental fast ion pressure profile versus time. DIII-D shot 96467.

Fig. 9 Frequency spectrum from TFTR. It shows the coupling between EPM (lower frequencies) and TAE with the same toroidal number n.

Fig. 10 Total energy vs. ICRF power in TFTR. Three regions can be identified: up to ~2.5 MW the increase is linear, no modes. From ~2.5 to ~4.0MW there is a slightly less increase with power; then for >4.0MW, as the TAE appear, definitely the energy rate of increase is lower. The amplitude of the EPM above 5 MW remains fairly constant.

AKNOWLEDGEMENTS.

One author (Bernabei) wishes to thank Drs. F. Zonca, L. Chen and J. Kramer for very enlightening discussions
Work supported by U.S. Department of Energy Contracts No. DE-AC02-76CH03073 and DE-AC03-99ER54463.

REFERENCES.

[1] PORCELLI, F., Plasma Phys. Controlled Fusion **33**,1601 (1991)

[2] BUDNY, R. V., BELL, M. G., JANOS, A. C. *et al.*, Nucl. Fusion **35**, (1995) 1497.

[3] GORELENKOV, N.N.,. CHANG, C. Z., and TANG, W. M., Phys. Plasmas **5**, (1998) 3389.

[4] BERNABEI, S., BELL, M.G., BUDNY, R.V., et al., Phys. Rev. Lett. **84** (2000) 1212.

[5] ZONCA,F., CHEN,L., Phys. Plasmas **3**, (1996) 323.

[6] COTTRELL, G.A., START, D.F.H, Nucl. Fusion **31** (1991) 61.

[7] HARVEY, R.W., McCOY, M.G. GA Report GA-A20978. Published in Proc. of Technical Committee Meeting on Advances in Simulation and Modeling of Thermonuclear Plasmas, Montreal, 1992, p. 489-526, IAEA, Vienna (1993).

[8] ST. JOHN, H., et al., in Plasma Physics and Controlled Nuclear Fusion Research, Seville, 1994 (IAEA, Vienna, 1995), Vol. 3, p. 603.

[9] PETTY, C.C., FOREST, C.B., BAITY, F.W., et al., Proc. Of 11th Topical Conf on Radio Frequency Power in Plasmas, AIP **355** (Palm Springs, 1995) 193.

[10] CHENG, C. Z., Phys. Reports 211, 1 (1992).

[11] WHITE, R. B., CHANCE, M. S., Phys. Fluids **27** 2455 (1984)

[12] WHITE, R. B., Phys. Fluids B **2** (4), 845 (1990)

[13] KRAMER, G.J., CHENG, C.Z., FU, G.Y., et al., Phys. Rev. Lett. **83**, 15 (1999) 2961

[14] BERNABEI, S., BELL, M.G., BUDNY, R.V., Phys. Of Plasmas **6**, no. 5 (1999) 1880.

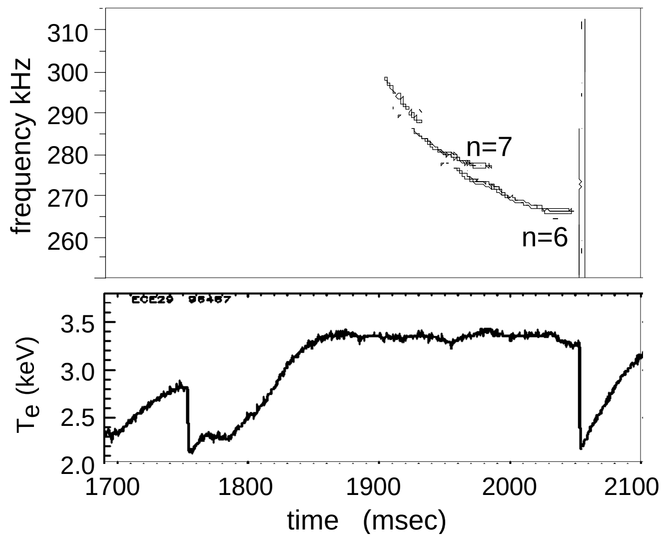

Bernabei Fig. 1

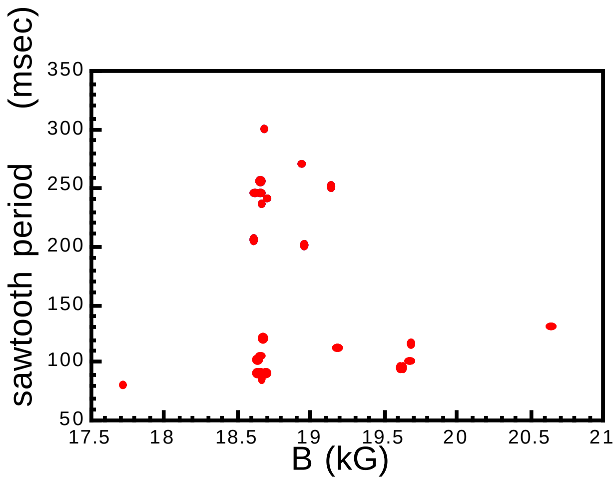

Bernabei Fig. 2

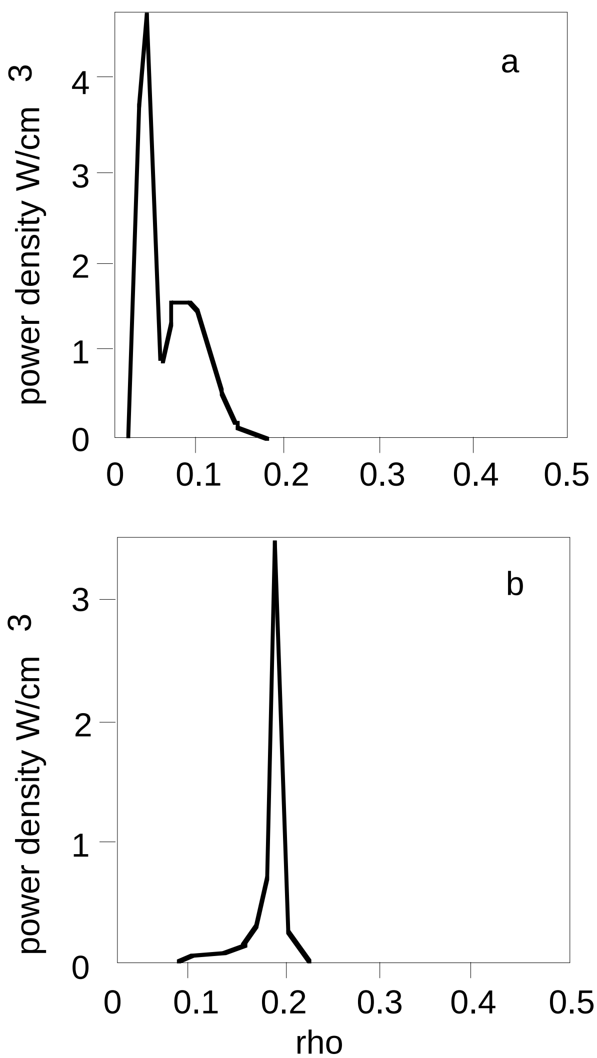

Bernabei Fig. 3

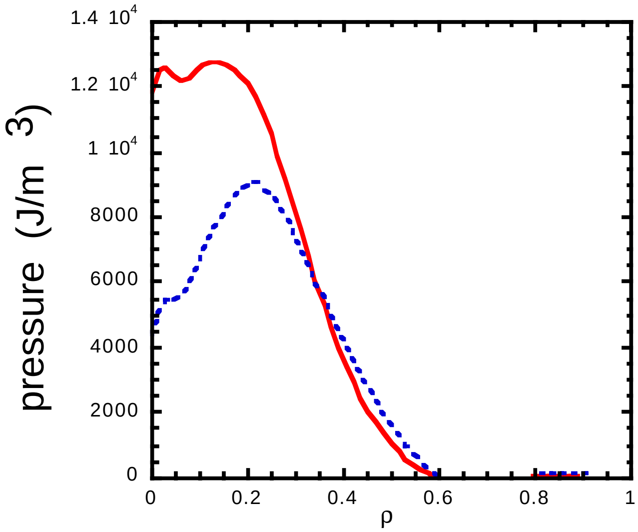

Bernabei Fig. 4

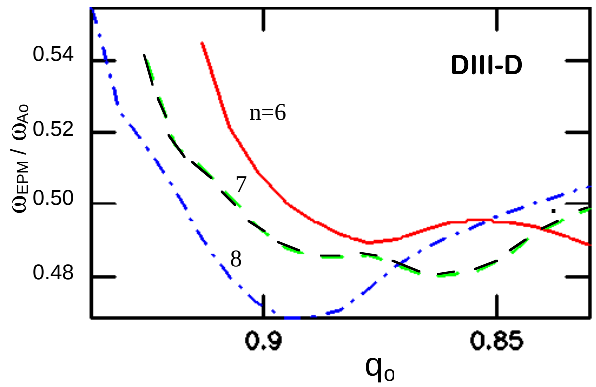

Bernabei Fig. 5

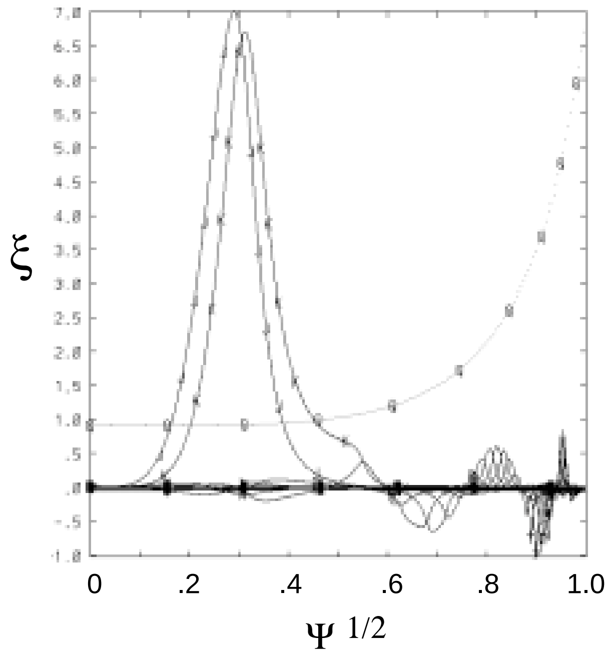

Bernabei FIG. 6

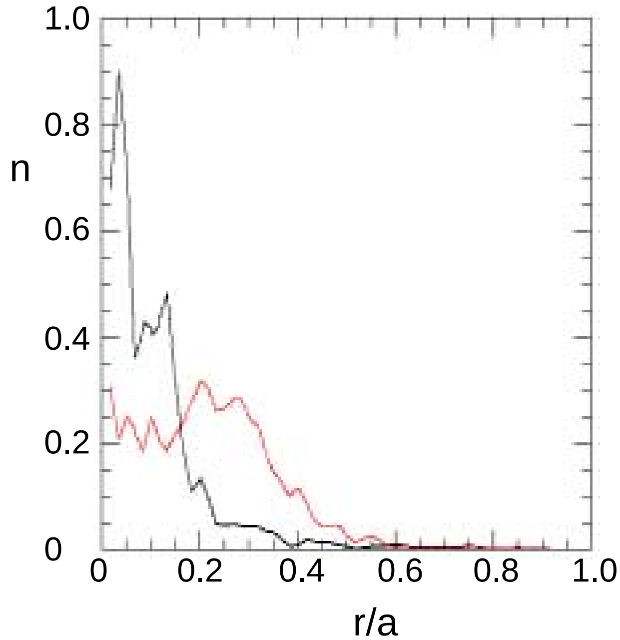

Bernabei Fig. 7

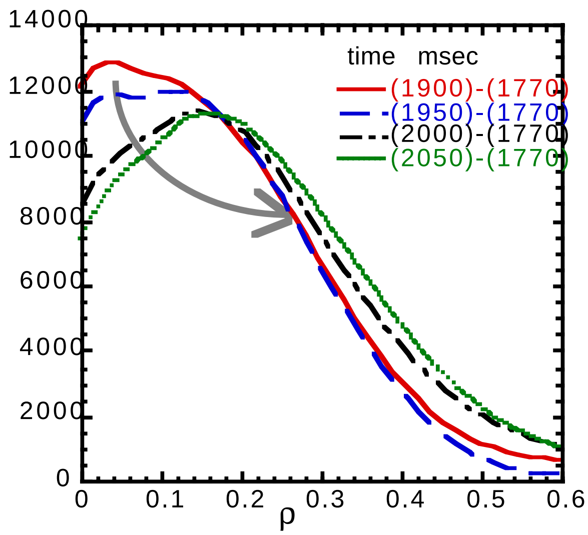

Bernabei Fig. 8

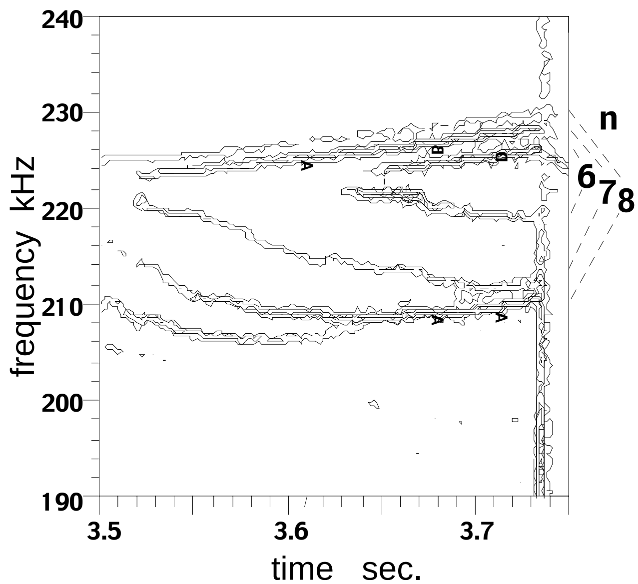

Bernabei Fig. 9

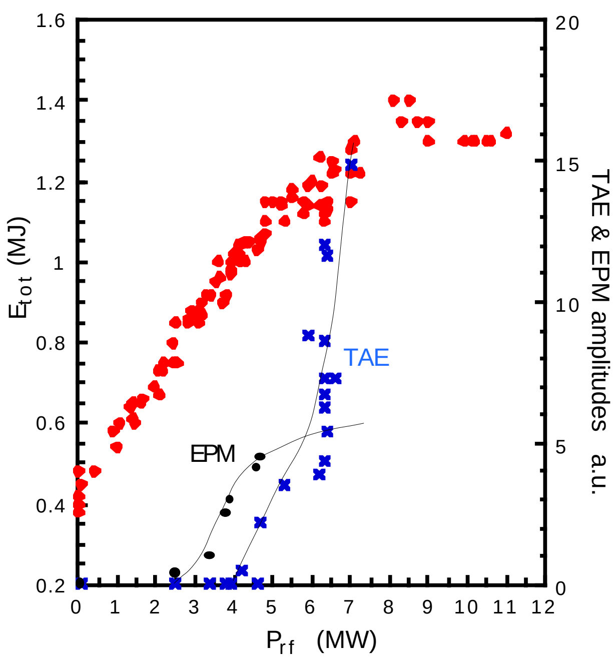

Bernabei Fig. 10

External Distribution

Plasma Research Laboratory, Australian National University, Australia
Professor I.R. Jones, Flinders University, Australia
Professor João Canalle, Instituto de Fisica DEQ/IF - UERJ, Brazil
Mr. Gerson O. Ludwig, Instituto Nacional de Pesquisas, Brazil
Dr. P.H. Sakanaka, Instituto Fisica, Brazil
The Librarian, Culham Laboratory, England
Library, R61, Rutherford Appleton Laboratory, England
Mrs. S.A. Hutchinson, JET Library, England
Professor M.N. Bussac, Ecole Polytechnique, France
Librarian, Max-Planck-Institut für Plasmaphysik, Germany
Jolan Moldvai, Reports Library, MTA KFKI-ATKI, Hungary
Dr. P. Kaw, Institute for Plasma Research, India
Ms. P.J. Pathak, Librarian, Insitute for Plasma Research, India
Ms. Clelia De Palo, Associazione EURATOM-ENEA, Italy
Dr. G. Grosso, Instituto di Fisica del Plasma, Italy
Librarian, Naka Fusion Research Establishment, JAERI, Japan
Library, Plasma Physics Laboratory, Kyoto University, Japan
Research Information Center, National Institute for Fusion Science, Japan
Dr. O. Mitarai, Kyushu Tokai University, Japan
Library, Academia Sinica, Institute of Plasma Physics, People's Republic of China
Shih-Tung Tsai, Institute of Physics, Chinese Academy of Sciences, People's Republic of China
Dr. S. Mirnov, TRINITI, Troitsk, Russian Federation, Russia
Dr. V.S. Strelkov, Kurchatov Institute, Russian Federation, Russia
Professor Peter Lukac, Katedra Fyziky Plazmy MFF UK, Mlynska dolina F-2, Komenskeho Univerzita, SK-842 15 Bratislava, Slovakia
Dr. G.S. Lee, Korea Basic Science Institute, South Korea
Mr. Dennis Bruggink, Fusion Library, University of Wisconsin, USA
Institute for Plasma Research, University of Maryland, USA
Librarian, Fusion Energy Division, Oak Ridge National Laboratory, USA
Librarian, Institute of Fusion Studies, University of Texas, USA
Librarian, Magnetic Fusion Program, Lawrence Livermore National Laboratory, USA
Library, General Atomics, USA
Plasma Physics Group, Fusion Energy Research Program, University of California at San Diego, USA
Plasma Physics Library, Columbia University, USA
Alkesh Punjabi, Center for Fusion Research and Training, Hampton University, USA
Dr. W.M. Stacey, Fusion Research Center, Georgia Institute of Technology, USA
Dr. John Willis, U.S. Department of Energy, Office of Fusion Energy Sciences, USA
Mr. Paul H. Wright, Indianapolis, Indiana, USA

The Princeton Plasma Physics Laboratory is operated
by Princeton University under contract
with the U.S. Department of Energy.

Information Services
Princeton Plasma Physics Laboratory
P.O. Box 451
Princeton, NJ 08543

Phone: 609-243-2750
Fax: 609-243-2751
e-mail: pppl_info@pppl.gov
Internet Address: http://www.pppl.gov